J|A|C|S
ARTICLES
Published on Web 02/20/2003

Self-Assembly of Fluid-Filled $KHCO_3$ Microfibers

Hugo Celio,[†] Jose Lozano,[†,§] Hyacinth Cabibil,[†,||] Lynette Ballast,[‡] and J. M. White*[,†]

Contribution from the Center for Materials Chemistry, Department of Chemistry and Biochemistry, University of Texas at Austin, Austin, Texas 78712-1167 and Advanced Micro Devices, Inc., Austin, Texas

Received December 9, 2002; E-mail: jmwhite@mail.utexas.edu

Abstract: Self-assembly of $KHCO_3$ fibers is observed when glassy oligomerized films of poly[(aminopropyl)-siloxane] containing K^+ ions, denoted K^+/poly-APS, are exposed to CO_2 and H_2O. The fibers are crystalline, narrow (0.4−3 μm diam), high aspect ratio (up to at least 300), and, on the basis of Raman spectroscopy, dominated by $KHCO_3$. The fibers contain fluid that is dominated by aqueous potassium formate (KOOCH). A multistep phenomenological model is proposed to account for the self-assembly.

Introduction

Among siloxanes, poly[(aminopropyl)siloxane] (poly-APS) is used as a coupling agent to bond inorganic to organic materials. Applications are found in microelectronics,[1] nanotechnology,[2] and biotechnology.[3] In biotechnology, for example, poly-APS is used to modify inorganic substrate surfaces to make them compatible with strands of DNA.[3] Adsorption and positioning of carbon nanotubes on electrode arrays has been achieved with the aid of poly-APS.[2] The broad appeal of poly-APS as a coupling agent and surface modifier stems, in part, from an extended oligomeric structure consisting of linear, cyclic, and cross-linked Si−O−Si polymeric networks.[1] Equally important is its bifunctionality, inorganic silanol (Si−OH), and organic aminopropyl groups ($-(CH_2)_3NH_2$). Under ambient conditions, a poly-APS film readily sorbs atmospheric CO_2 and H_2O by forming complexes, both carbamate−ammonium (reaction between $-NH_2$ and CO_2) and water−silanol (via hydrogen bonded interactions). Recent papers have addressed the rather complicated architecture of poly-APS and the orientation and reactivity of its functional groups.[4]

In this paper, we investigate poly-APS thin films containing K^+ ions, the latter adding a third functionality, ionic interactions. These can act as counterions to stabilize the formation of anions such as bicarbonate (HCO_3^-), formate ($HCOO^-$), and ionic groups (e.g., SiO^--K^+) of the poly-APS films. We report, for the first time, self-assembly of crystalline potassium bicarbonate into microtubes filled with aqueous potassium formate.

In two recent papers, we reported that the structural, chemical, and mechanical properties of 50 nm thick poly-APS films (no added alkali ions) deposited on soda lime glass and on SiO_2/Si(100) were strikingly different.[5,6] Highly organized 2D nanoribbons (height ≈ 3 nm, width ≈ 8 nm, and variable lengths exceeding 20 μm) self-assembled on soda lime glass but not on SiO_2/Si(100).[5] The self-assembly was correlated to two critical parameters, Na^+ leached from the glass and H_2O and CO_2 absorbed from the ambient atmosphere. Interestingly, the mechanical properties of the two films were quite different; the elastic modulus, measured by interfacial force microscopy, of the poly-APS film on glass was 4× smaller than that on SiO_2/Si(100).[6] The lower modulus on soda lime glass was attributed to an acid−base reaction involving Na^+ that breaks some Si−O−Si bonds in poly-APS, reducing the force required to deform the film. To account for the self-assembly and nanomechanical properties, we proposed that the nanoribbons were composed of mobile and small poly-APS oligomers capped with a carbamate salt, $(-NHCOO^-)Na^+$, or with protonated NH_3^+ functional groups. These ionic species, we suggested, directed the self-assembly of the nanoribbons via hydrogen bonding and electrostatic interactions.[5,6]

Interference from the relatively large background and our inability to separate them from the matrix precluded direct chemical analysis of the nanoribbons. In an attempt to circumvent this problem and simplify the system, thicker films, ∼40 μm, were prepared by placing on oxidized Si(100), rather than soda lime glass, a homogeneous solution of poly-APS. The solution was prepared by mixing water with γ-aminopropyl triethoxysilane and doping it with KOH. As H_2O and C_2H_5OH evaporated, this film gelled, and upon exposure to CO_2 and H_2O, novel crystalline, micron-diameter, high aspect ratio tubular structures (fibers) formed that were filled with fluid. Direct spectroscopic evidence is provided for the tubes being crystalline $KHCO_3$ and the fluid being dominated by aqueous KOOCH.

[†] University of Texas at Austin.
[‡] Advanced Micro Devices, Inc.
[§] Present address: Dept. of Physics, Bradley University, Peoria, IL.
[||] Present address; 3M Corp., St. Paul, MN.

(1) (a) Plueddemann, E. P. *Silane Coupling Agents*; Plenum Press: New York, 1982. (b) *Silanes and Other Coupling Agents*. Mittal, K. L., Ed.; VSP: The Netherlands, 1992. (c) Ishida, H. In *The Interfacial Interactions in Polymeric Composites*; Kluwer Academic Publishers: Norwell, MA, 1993; Chapter 8.
(2) Lewenstein, J. C.; Burgin, T. P.; Ribayrol, A.; Nagahara, L. A.; Tsui, R. K. *Nano Lett*. **2002**, *2*, 443.
(3) Umemura, K.; Ishakawa, M.; Kuroda, R. *Anal. Biochem.* **2001**, *290*, 232.
(4) White, L. D.; Tripp, C. P. *J. Colloid Interface Sci.* **2000**, *232*, 400.
(5) Cabibil, H.; Pham, V.; Lozano, J.; Celio, H. White, J. M.; Winter, R. *Langmuir* **2000**, *16*, 10471.
(6) Cabibil, H.; Celio, H.; Lozano, J.; White, J. M.; Winter, R. *Langmuir* **2001**, *17*, 2160.

10.1021/ja021419n CCC: $25.00

The poly-APS plays a critical role in self-assembly; in its absence, only the long-known nucleation and growth of needle-like and rhombohedral crystals of $KHCO_3$ are observed.[8] The fiber formation process has attributes similar to the growth of $CaCO_3$ on organic Langmuir monolayers.[7] To account for formate, we propose a reaction involving conversion of bicarbonate ions into formate ions catalyzed by K^+/poly-APS.[9]

Experimental Section

Unless specified otherwise, the experiments were carried out at ambient laboratory temperature (25 ± 4 °C), relative humidity (50 ± 20%), and pressure (1 ± 0.05 atm). The substrates (2 × 1 cm^2) were cut from microelectronic grade Si(100) wafers covered with ~2 nm of native oxide and were cleaned by standard methods.[5,6] These substrates were very flat; the rms roughness, measured by atomic force microscopy, was 0.20 ± 0.02 nm.

The film precursor solution was prepared by mixing 1.5 g of γ-aminopropyl triethoxysilane (γ-APS, 99% purity, Aldrich Chemical Co.) with 28.5 g of high purity H_2O (Milli-Q; 18 MΩ). Hydrolysis and oligomerization forms poly-APS, a clear homogeneous solution with pH = 10.5.[5] The pH is controlled by protonation of the amine group of the poly-APS; that is, $-NH_2 + H_2O \leftrightarrow -NH_3^+$ and OH^-.[1] After the solution was stirred for 10 min, 0.17 g of solid KOH (EM Science) was added, increasing the pH to 11.6.

For most experiments, a 0.4 g droplet of this K^+/poly-APS solution was placed onto a SiO_2/Si(100) surface that was then placed within a loosely covered Fluoroware container. The droplet wet the substrate and within 12 h, gelation occurred to form a clear, uniform, glassy film. After 24 h, the films were transferred to a second container and exposed for 30 s to a stream of cool CO_2 (273 K; flow rate 4 std cc min^{-1}; Matheson, purity 99.9%). During the subsequent return to the Fluoroware container under ambient air, water (<5 μm thick) condensed on the cool film surface, and the film thickened by ~ 50%, fractured, and, in many places, delaminated from the SiO_2/Si(100) substrate. Fiber growth typically commenced within 24 h.

Two other procedures also led to fibers: (1) exposure of glassy films to ambient air and (2) bubbling CO_2 into the K^+/poly-APS solution before placing a droplet onto a substrate. The latter solution, denoted *carbonated* K^+/poly-APS, was prepared by bubbling CO_2 (4 std cc min^{-1}) until the pH decreased to 7.6. The pH drops because of reactions that form H^+ and HCO_3^- and carbamate (−NHCOOH), the latter due to carboxylation of the amines of poly-APS. The induction times were longer, the initial growth rates were slower, but the asymptotic fiber lengths were longer (some exceeding 1000 μm) for these two procedures compared to the procedure described in the previous paragraph.

For analysis, fibers were removed and placed on various substrates using a silicon nitride cantilever (Thermomicroscopes) linked to a micromanipulator (1 μm spatial resolution, Zeiss, Co.). A tungsten tip, controlled with the micromanipulator, was used to bend and fracture fibers. The removal, bending, and fracturing were monitored with a confocal microscope (magnification 200×) and recorded with a video camera. Four substrates were used: Teflon (0.08 mm thick), highly oriented pyrolytic graphite (HOPG, SPI Supplies), 200 nm SiO_2 on Si(100), and gold deposited on mica.[10] To confirm the composition of the fibers and the fluid, reference samples of potassium bicarbonate (Mallinckrodt, 99% purity) and potassium formate (Aldrich, 99% purity) were examined.

Reflection mode optical micrographs of the films and fibers were taken using a microscope (BX60 Olympus) equipped with crossed polarizers and a digital camera (Diagnostics). Atomic force microscope (AFM) measurements were performed using a CP Research Autoprobe (Thermomicroscopes, Sunnyvale, CA) operated in the noncontact (NC-AFM) mode. Fibers removed and placed on HOPG were examined by scanning electron microscopy (SEM LEO 1530) and energy-dispersive X-ray spectrometry (EDS).[11] Fibers on Teflon were examined by X-ray photoelectron spectra (XPS) using a Physical Electronics (PHI) model 5700 ESCA spectrometer with an Al monochromatic source (Al Kα energy of 1486.6 eV).[5] All high-resolution scans used a takeoff angle of 45° and pass energy of 11.75 eV. The C(1s) binding energies (BE) of Teflon and bicarbonate, HCO_3^-, were fixed at 292.9 and 290.2 eV, respectively.[12] Micro-Raman spectra (488 nm Ar^+ laser operated with a 2 μm diameter beam and 6 mW incident power) of fibers on a gold surface were recorded (180° backscattered geometry) using a Renishaw Raman System 2000 spectrometer coupled to a Leica INM200 microscope with a 50× objective and a charge-coupled device (CCD) detector (Wright Instruments Ltd).

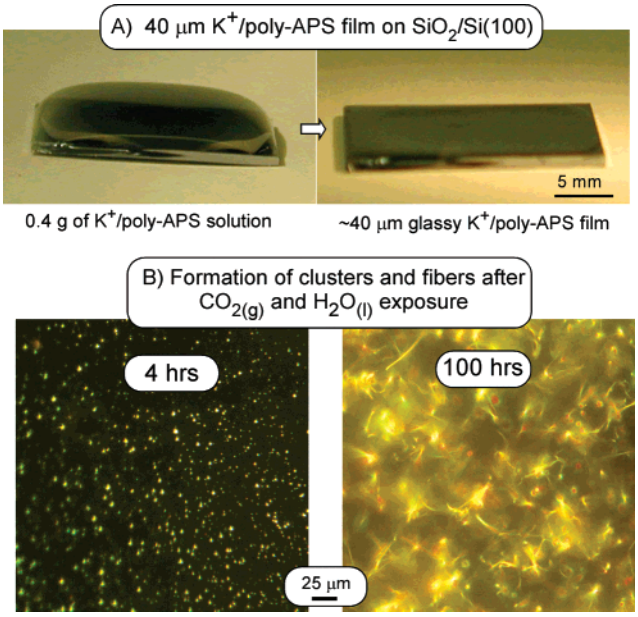

Figure 1. The top panel (A) shows optical microscope images illustrating the conversion of a droplet of liquid solution into a glassy 40 μm thick K^+/poly-APS film on SiO_2/Si(100). The lower panel (B) is a microscope image of the formation of clusters (4 h), followed by fibers (100 hr) after exposure to $CO_{2(g)}$ and $H_2O_{(l)}$.

Results

Evidence for Self-Assembly of High Aspect Ratio Fibers. Two optical microscope images, one taken immediately after placing a 0.4 g droplet of K^+/poly-APS onto a clean SiO_2/Si-(100) and the second, after 12 h in ambient air, top panel of Figure 1, show that the droplet wets the surface, becomes thinner as the water and ethanol evaporates, and forms a glassy film that is, in this case, 40 μm thick. At higher spatial resolution (AFM), there are micron-sized pores and/or depressions (not shown). After exposure to $CO_{2(g)}$ and $H_2O_{(l)}$, the film thickens and optical microscopy (bottom panel of Figure 1) shows a nonuniform distribution of bright spots within 4 h and fibers after 100 h.

Figure 2 shows linear and cross-polarized optical micrographs (500× magnification) of an area where a single fiber and the film surface are simultaneously in focus; other fibers are not in focus and typically tilt 70 ± 15° with respect to the surface

(7) Archibald, D. D.; Qadri, S. B.; Gaber, B. P. *Langmuir* **1996**, *12*, 538.
(8) (a) Nitta, I.; Tomiie, Y.; Koo, C. H. *Acta Crystallogr.* **1952**, *5*, 292. (b) Pedersen, B. *Acta Crystallogr.* **1968**, *B24*, 478. (c) Thomas, J. O.; Tellgren, R.; Olovsson, I. *Acta Crystallogr.* **1974**, *B30*, 2540.
(9) Celio, H.; White, J. M. Manuscript in preparation.
(10) Poirier, G. E.; Fitts, W. P.; White, J. M. *Langmuir* **2001**, *17*, 1176.
(11) http://www.leo-em.co.uk/SEMPRODUCTS/Leo1530.htm.
(12) *Handbook of X-ray Photoelectron Spectroscopy*. Physical Electronics Inc.: Eden Prairie, MN, 1995.

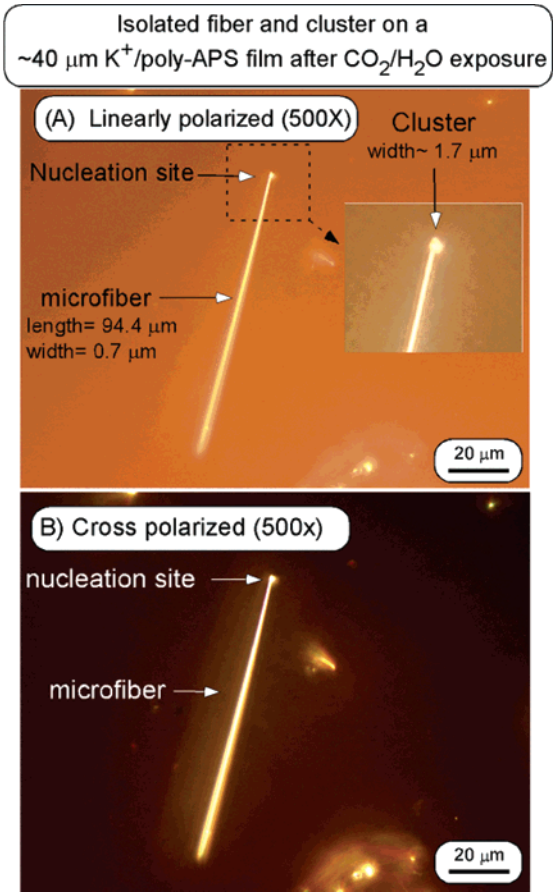

Figure 2. Optical microscope images (500×) of an isolated self-assembled fiber taken with (A) linearly polarized light and (B) cross-polarized light. A straight fiber (uniform 0.7 μm diameter and 97.4 μm long) emerges from a nucleation site located on the surface of the K^+/poly-APS film. The inset is a magnified and focused region of the nucleation site. In image B, the bright field produced by the fiber and nucleation site indicates that both are crystalline, whereas the dark field indicates an amorphous noncrystalline structure.

normal. This fiber is straight, long (94 μm), uniformly narrow (0.7 μm cross-section), and crystalline. The point at which the fiber emerges from the surface is significant; the inset indicates a crystalline region with a diameter (1.7 μm) that is larger than the fiber. Other bright regions reflect crystalline material at and beneath the film surface.

A *carbonated* K^+/poly-APS film exposed to ambient air also exhibits fibers (Supporting Information). The areal number density is about the same but the fibers are longer (up to at least 10^3 μm) and are often curved in this procedure compared to the standard procedure. In addition, needlelike crystals appear frequently. Occasionally, a micron-sized rhombohedral crystal is found. As an important reference, a droplet of aqueous $KHCO_3$ deposited on a substrate in the absence of poly-APS formed needles and rhombohedra but no fibers.[8] Dependent on the procedure used, slow fiber growth has been observed for periods as long as seven months.

Underscoring the importance of film thickness, we did not observe the fibers when they were 1000-fold thinner, ~50 ± 10 nm. Films were prepared by spin-coating poly-APS solution doped with KOH and CO_2 onto SiO_2/Si(100); rather, nanoribbons (not shown) were observed, consistent with our earlier report.[5]

Evidence for Alkali Bicarbonate Fibers and Formate Fluid. Micro-Raman spectra of fibers removed from a K^+/poly-APS film and placed on a gold foil were indistinguishable from spectra of polycrystalline $KHCO_3$, Figure 3. The band positions and line shapes of all fundamental transitions for the fiber (spectrum A) and the reference (spectrum B) are identical within experimental error and are in accord with literature values for $KHCO_3$ (Table 1). In addition, the overtone and combination bands at 1820, 2800, 2927, and 3116 cm^{-1} are also in excellent agreement with data for crystalline $KHCO_3$,[13] a crystal structure that involves dimers (inset of Figure 3).[13a]

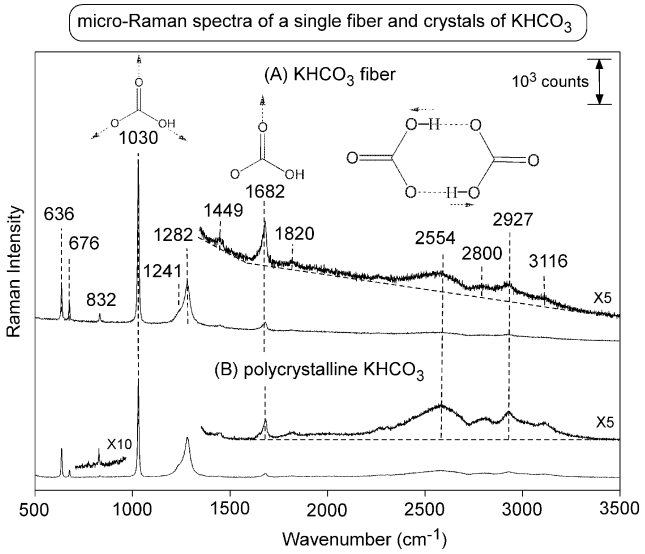

Figure 3. Micro-Raman spectra (500−3500 cm^{-1}) of (A) a single fiber transferred to a gold substrate and (B) a reference sample of polycrystalline $KHCO_3$. The closely matching features identify the fiber as dominated by crystalline $KHCO_3$.

Table 1. Vibrational Frequencies (cm^{-1}) of Crystalline $KHCO_3$ and a Microfiber

	band	crystalline $KHCO_3$[a]	microfiber[b]	band assignment[a]
A_g	ν_1	2590 (s)	2554	ν(O—H)
	ν_2	1682 (m)	1682	ν(C═O)
	ν_3	1448 (w)	1449	δ(O—H···O)
	ν_4	1283 (s)	1283	ν(C···O) + ν(C═O)
	ν_5	1029 (s)	1030	ν(C═O) + ν(C···O)
	ν_6	676 (w)	676	$\delta(O_1C{=}O_2)$ + ν(C═O)
	ν_7	635 (s)	636	δ(C═O)

[a] Reference 13. [b] This work; s = strong, m = medium, w = weak.

The strongest band in Figure 3 (1030 cm^{-1}) is assigned to the coupled symmetric stretch of (C···O) and (C═O). The non-hydrogen-bonded oxygen (inset) is covalently bound to carbon and approximates a carbon-to-oxygen double bond (1682 cm^{-1}). The energy of this mode lies in the range (1650−1750 cm^{-1}) found for the C═O stretch in aldehydes and ketones.[14] The hydrogen bonds, O—H···O, of $KHCO_3$ are delocalized compared to isolated O—H groups, resulting in a relatively low (2554 cm^{-1}) and broad (fwhm = 177 cm^{-1}) O—H stretching region typical of hydrogen-bonded carboxylic acids.[14] From Figure 3 and Table 1, we conclude that the fibers are dominated by crystalline $KHCO_3$.

Raman analysis of an *undetached* $KHCO_3$ fiber growing out from the edge of a piece of the K^+/poly-APS film reveals

(13) (a) Nakamoto, K.; Sarma, Y. A.; Ogoshi, H. *J. Chem. Phys.* **1965**, *43*, 1177. (b) Oliver, B. G.; Davis, A. R. *Can. J. Chem.* **1973**, *51*, 698.
(14) Nakamoto, K. *Infrared and Raman Spectra of Inorganic and Coordination Compounds*; John Wiley: New York, 1997.

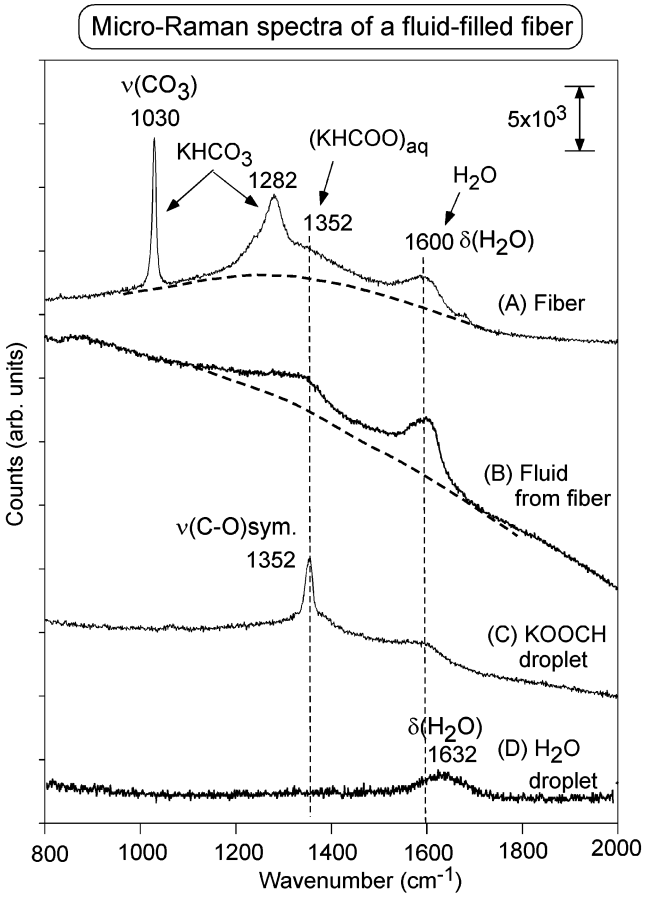

Figure 4. Micro-Raman spectra (800−2000 cm^{-1}) of (A) a single fiber that is bonded to a K^+/poly-APS film but viewed to eliminate the film contribution, (B) a fluid droplet from a fractured fiber, (C) a droplet of potassium formate solution, $KOOCH_{(aq)}$, and (D) pure H_2O. All samples were supported on a gold substrate. The closely matching features identify the fluid-filled fiber as dominated by crystalline $KHCO_3$ and fluid-phase KOOCH.

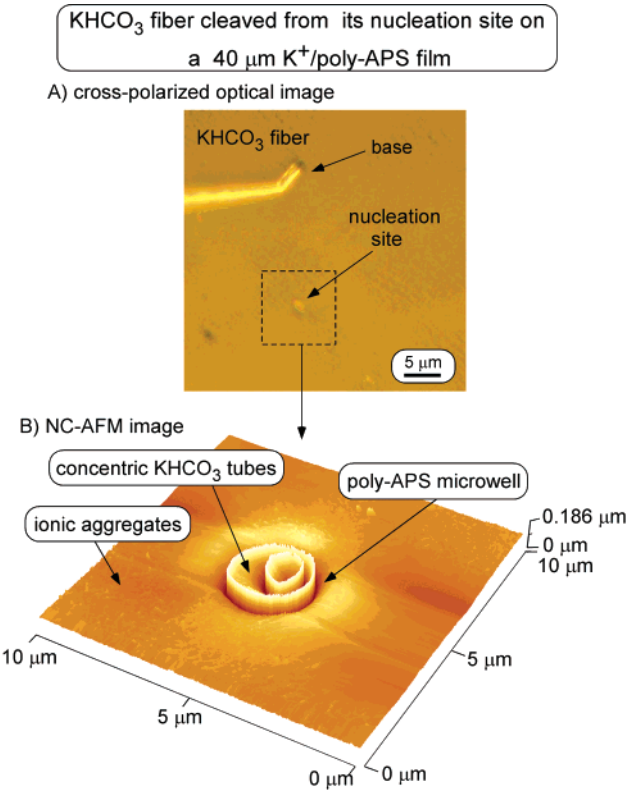

Figure 5. Optical (top) and AFM (bottom) images associated with a single $KHCO_3$ fiber that self-assembled after exposure of a 40 μm K^+/poly-APS film to ambient air. After 3 months in ambient air, a micromanipulator was used to mechanically cleave the fiber and move it away from its nucleation site. In Figure 6A, a cross-polarized optical image (500× magnification) shows the $KHCO_3$ fiber (175 μm long and 1.8 μm wide) that was cleaved and moved approximately 20 μm away from its original position (center of dashed square). The (10 × 10 μm^2) AFM image (B) of the dashed square region from part A shows the cylindrical and funnel-shaped nature of the structure at the position where the fiber emerged from the film. In the surrounding region, small features attributed to ionic aggregates are evident.

additional molecular components, Figure 4A. To avoid contributions from the film, this image was taken more than 20 μm away from the film edge. The spectrum differs from that of the detached fiber, Figure 3, in the 800−2000 cm^{-1} region. The bands at 1030 and 1282 cm^{-1}, but not those at 1352 (shoulder) and 1600 cm^{-1}, are attributable to $KHCO_3$. When the fiber was fractured, fluid appeared on the gold substrate, and the Raman spectrum of this fluid (Figure 4B) clearly shows the two broad bands of spectrum A but no evidence for $KHCO_3$.

For comparison, droplets of saturated potassium formate solution, $KOOCH_{(aq)}$, H_2O/KOOCH = 4, and of H_2O were examined (Figure 4C and D). The 1352 cm^{-1} band is assigned to the symmetric C−O stretching mode of formate,[15] and the 1600 cm^{-1} component to the bending mode of water, perturbed by interaction with formate ion, $CHOO^-$, that is, the bending mode of pure water at 1632 cm^{-1} (D), is downshifted by the hydrogen-bonding interactions between water and formate ions. The full width half-maximum (fwhm) of the 1352 cm^{-1} band in spectrum B is 10× broader than that in spectrum C. This is attributed to interactions between H_2O and $CHOO^-$. The H_2O/$CHOO^-$ ratio must be relatively small (<7), since $KHCO_3$ crystals (e.g., needles and rhombohedra) dissolve if this ratio exceeds 7. Relevant to the long-term growth of the fluid-filled fibers, we find that solid $KHCO_3$ remains stable indefinitely in concentrated aqueous KOOCH (at least several months).

The source of formate ($HCOO^-$) ions is currently under investigation. One plausible source is a reaction involving the interaction of the aminopropyl group of poly-APS with HCO_3^- to form an intermediate that decomposes to $HCOO^-$ and a hydroxylamine functionalized poly-APS moiety. Preliminary micro-Raman and XPS analysis[9] indicates that formate ions do form slowly when a saturated potassium bicarbonate solution is spin-coated onto a previously formed thin (50 ± 10 nm) undoped poly-APS film. First, micron-sized clusters of solid $KHCO_3$ formed. Second, after exposure to ambient air for 24 h, $KHCO_{3(aq)}$ spread around the perimeter of the cluster, forming a thin layer of $KHCO_3$ over the poly-APS. Within a week, fibers emerged from this perimeter region. After several weeks, the solid $KHCO_3$ microclusters were replaced by droplets of very stable fluid. A micro-Raman spectrum of the fluid is indistinguishable from that of Figure 4C, the latter prepared by exposing dry and pure $KOOCH_{(s)}$ to ambient air. $KOOCH_{(s)}$ is very hygroscopic and under our typical laboratory conditions forms a stable solution with a molar ratio H_2O/KOOCH = 4.

Evidence for Tubular Fibers. Having identified that fibers are crystalline $KHCO_3$ and that some of them also involve $KOOCH_{(aq)}$, we turn to AFM of areas from which fibers emerge (Figure 5). A detached fiber and the site (slightly out-of-focus)

(15) Heyns, A. M. *J. Chem. Phys.* **1986**, *84*, 3610.

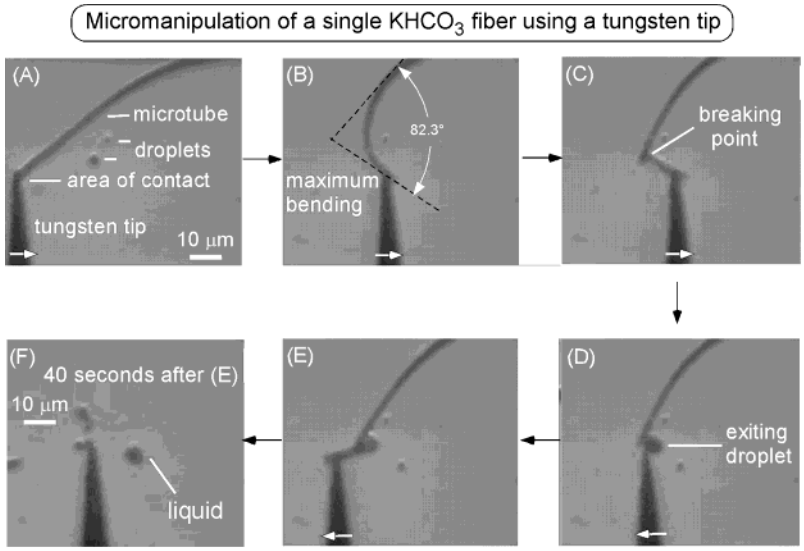

Figure 6. Sequential optical images (clockwise from image A) showing micromanipulation, using a tungsten tip, of a 3.5 μm wide $KHCO_3$ fiber attached at one end to a bundle of fibers in a SiO_2/Si(100) substrate. The direction taken by the W tip is indicated in each frame by a white arrow. When the tip is moved from left to right (A−C), the fiber is transformed from its straight shape (A) into a curved configuration (B) that fractures near the W tip (C). When the tip is moved in the reverse direction (D−F), a fluid droplet appears at the break point (D). The droplet emerges from the smaller fragment (E and F). The 10 μm bar in image A is valid for all images.

from which it grew are identified in Figure 5A. The cross-polarized optical image (500× magnification) shows a 2.5 μm wide short section and a kink near the fiber base followed by a long straight section of uniform diameter (1.8 μm). The tubular character is evident, particularly in the short section.

An AFM image of the site from which the tube emerged, Figure 5B, possesses cylindrical symmetry, suggesting concentric $KHCO_3$ structures, 2.5 μm and 1.0 μm diam, respectively, surrounded by a funnel-shaped structure with a diameter of 4.0 μm at the surface and 2.5 μm at the bottom. The latter is the same as the diameter of the outer tube and the short section of the detached fiber, suggesting that the structure at the bottom may serve as a template for the emerging fiber and that the wall thickness of the tubular fiber is ~0.7 μm. We speculate, but cannot prove, that the funnel-shaped region is associated with one of the depressions in the glassy K^+/polyAPS film. Throughout the region surrounding the funnel, there are small structures (bright spots) that we attribute to ionic aggregates.

Evidence for Fracture of Fibers and Stable Fluid within Them. Bending a fiber reveals mechanical properties and provides direct evidence for fluid within. In this experiment, a 3.5 μm diameter fiber was transferred to a clean SiO_2/Si(100) substrate and positioned so that one end contacted the micromanipulator W tip (radius = 0.75 μm)[5,6] while the other end was attached to a bundle of fibers. When videoing a fiber being bent, the fluid contained within is evident as movement of material along the fiber axis (not shown).[16] Selected frames from the video are shown in Figure 6. As the tip moves from left-to-right in passing from frame A to B, the fiber is elastically stressed; that is, upon reversing directions, it returns to configuration (A). Beyond the elastic limit, fracture occurs (C), and as the tip reverses, a droplet of fluid emerges (D). As the tip carries the small fragment away (E) and the long fragment moves out the image (F), the droplet (7 μm dia) remains behind (F).

While the time scale required for the solidification of these droplets was not established, the two liquid droplets in Figure 6A are a result of prior tube fractures from the bundle of fibers and, thus, have remained liquid for at least the 10 min required to take the remaining images. This is consistent with the fluid being dominated by $KOOCH_{(aq)}$, as proposed on the basis of Figure 4, and inconsistent with a saturated aqueous solution of $KHCO_3$; that is, the latter begins to form solid $KHCO_3$ on this time scale.

The internal diameter of the fractured portion of the fiber could not be determined with optical microscopy; however, additional frames (not shown) taken during the reverse motion (D to F) show that the short (20 μm) fragment released the observed fluid. Assuming a cylindrical tube that is completely emptied of fluid upon fragmentation, assuming the droplet and fragment have the same density, and assuming the droplet forms a dome with a 4 μm radius and 2 μm height, we estimate the inside diameter of this fractured tube is 1 μm. This estimate is similar to that obtained for the cleaved fiber of Figure 5.

Evidence for Fibers Originating Deep within the Film. In an edge view of a film, Figure 7, two fibers are identified. Fiber #1 (110 μm long and 0.8 μm wide) is in focus and is oriented with its long axis perpendicular to the film surface. Fiber #2 (65 μm long and roughly 1 μm wide) is out-of-focus because its long axis is tilted 45 ± 15° with respect to the surface normal. The magnified section (Figure 7B) clearly evidences that fiber #1 originates at least 10 μm below the surface of this 30 μm thick film. The structure near the origin of these fibers could not be determined.

Evidence for Growth Rates. Rates of fiber growth at ambient conditions were examined by imaging the edge of a film along a direction normal to the film surface, Figure 8, for various elapsed times after dosing $CO_{2(g)}$ and $H_2O_{(l)}$. Consistent

(16) For another fiber, the W tip was positioned perpendicular to the longitudinal direction of the fiber. With the tip in contact with and slowly moving along the longitudinal direction of the fiber, we observed motion of the fluid inside the tube.

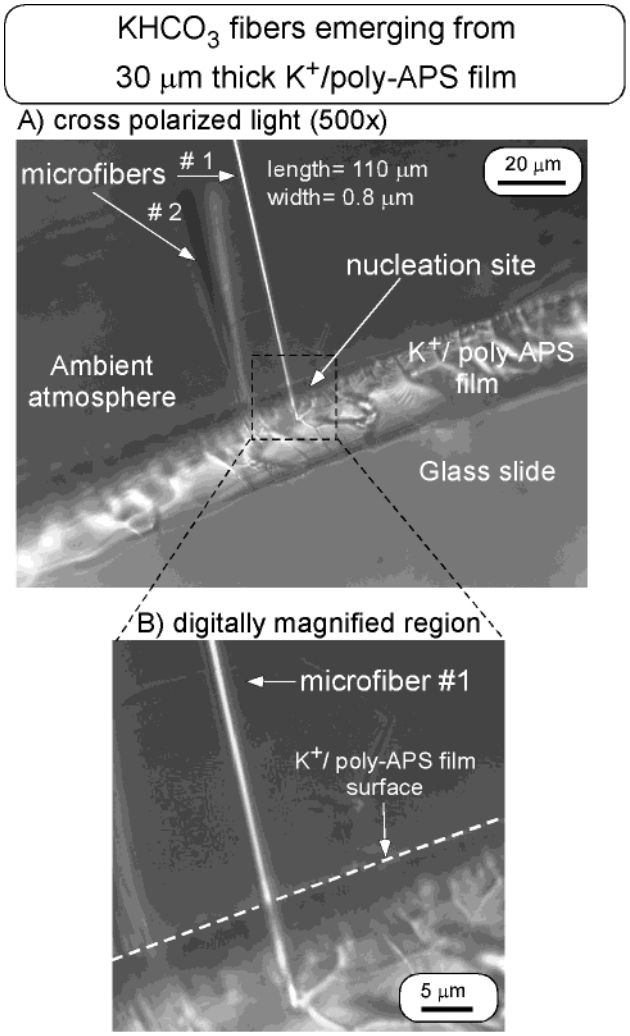

Figure 7. Cross-polarized optical edge view of a 30 μm thick K^+/poly-APS film. Two $KHCO_3$ fibers (#1 and #2) are marked. Fiber #1 is in focus and originates deep within the film (B).

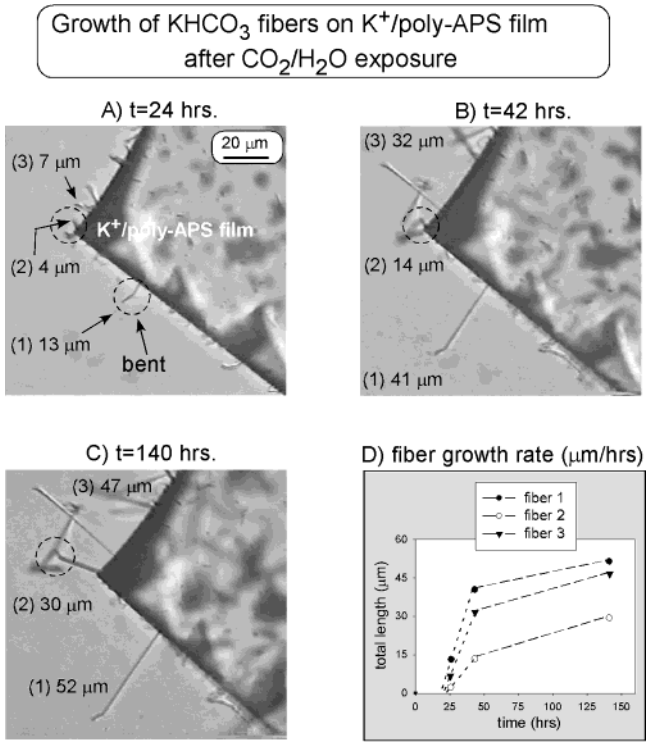

Figure 8. As a function of elapsed time, three optical images taken from looking down across the edge of a K^+/poly-APS film supported on a glass slide after exposure to cool CO_2 and condensation of a thin H_2O layer (see text): (A) 24 h, (B) 42 h, and (C) 140 h. Fibers on these edges tend to grow with their cylinder axes parallel to the surface of the film. Panel D plots the total length of each fiber as a function of elapsed time.

with Figure 1, no fibers are evident for at least 4 h, but large numbers ($\sim$50) are present after 24 h (Figure 8A). Between 24 and 42 h, most fibers grew rapidly and very few new fibers emerged. Between 42 and 140 h, growth slowed markedly. The time-dependent length of three marked fibers (Figure 8D) illustrates, and linear extrapolation, using the 24 and 42 h data, predicts an onset of time of 21 ± 2 h for all three. The diameter of each fiber is about 1 μm, but lengths varied from 4 to 14 μm after 24 h. Interestingly, between 42 and 140 h, each fiber added 14 ± 2.5 μm. The following phenomenological picture emerges: The initial system formed by dosing a K^+/poly-APS film with CO_2 and H_2O undergoes relatively slow structural changes before fibers nucleate. These structural changes occur relatively uniformly over time to form structures of a certain size, so that fiber nucleation times do not differ more than 10% and fiber diameters do not differ more than a factor of 2. Once nucleated, fibers initially grow relatively rapidly and at different rates, but then growth rates slow and become much more uniform. As noted previously, growth can extend for periods of months, likely limited by the availability of fluid.

Evidence for Where Material Is Added To Elongate the Fiber. The kink in fiber #1 of Figure 8 moves away from the surface with time, suggesting that new material is being added at its origin within the film. On the other hand, the behavior of fiber #2 might suggest adding new material at either end of the fiber, perhaps during different stages of the growth. This is taken as evidence for film growth at the terminus and is supported by images of a fiber prepared using *carbonated* K^+/poly-APS (not shown). Over seven months, a bend remained fixed near the surface, while the fiber grew to a length of 1000 μm. Over all but the last 100 μm, the diameter remained constant (4 μm). The diameter near the terminus was smaller by a factor of 2. Thus, proposed models describing fiber growth must account for adding material at either end.

Further Evidence from SEM, EDX, and XPS. SEM, EDX, and XPS data were used to complement the optical microscopy, atomic force microscopy, and Raman spectroscopy. SEM micrographs of fibers grown from a *carbonated* K^+/poly-APS solution (Supporting Information) display areas densely populated with straight and curved fibers. Damage occurs rapidly even at electron beam energies of 250 eV precluding higher magnification. The detailed conditions leading to straight or curved fibers remain unknown.

In a separate experiment, a bush-like bundle of fibers was examined by SEM and EDS (Supporting Information) after removal from the carbonated K^+/poly-APS film and transfer to a clean highly oriented pyrolytic graphite (HOPG) substrate, the latter selected for high conductivity and minimal impurity levels. The bundle contains at least 50 entangled fibers with lengths ranging from 45 to 150 μm and widths from 1.3 to 2.0 μm. EDS (Supporting Information) shows evidence for K and O with contributions consistent with reference $KHCO_3$ (intensity ratio, $O/K = 1.27 \pm 0.05$ for both). Consistent with, at most,

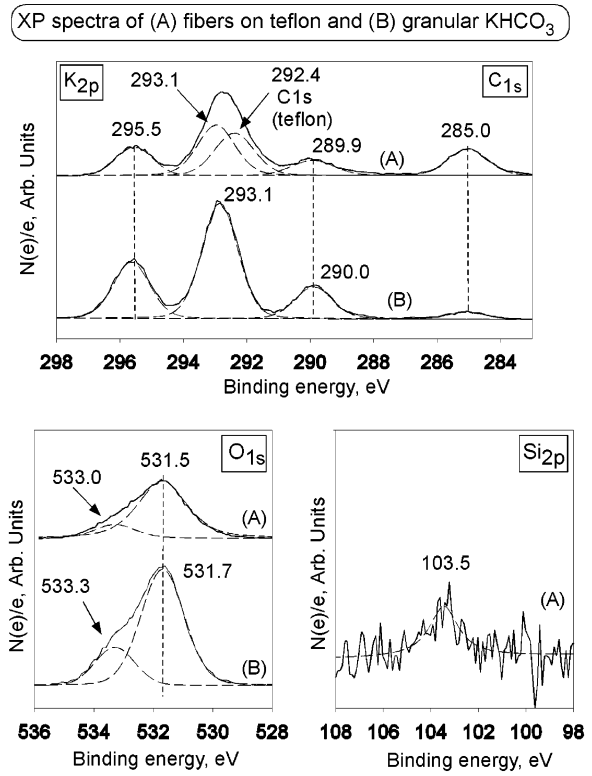

Figure 9. XPS of (A) fibers transferred from K^+/poly-APS onto Teflon and (B) reference granular $KHCO_3$. Upper panel, C(1s) and K(2p); lower left panel, O(1s); and lower right, Si(2p) regions. The C(1s) peak of Teflon was fixed at 292.4 eV BE.

small contributions from poly-APS, there is no evidence for Si (<1 atom %).

Another bundle was examined by XPS after transfer to a Teflon substrate, curves labeled A in Figure 9. When the fibers on Teflon are compared with a $KHCO_3$ reference, curves labeled B, the spectra are equivalent, with two exceptions. First, and most significant, there is a weak Si(2p) signal from the fibers that is absent in the reference, $KHCO_3$. Second, the 285.0 eV BE peak in the C(1s) panel is not the result of X-ray induced chemistry;[17] rather, it is attributed to C(1s) of hydrocarbon species and is relatively stronger for the fibers. The other signals are those expected for Teflon C(1s) at 292.4 eV,[12] for K(2p) at 293.1 and 295.5 eV,[12] for C(1s) and O(1s) of bicarbonate at 290.1 and 531.7 ± 0.1 eV, respectively, and for O(1s) of H-bonded bicarbonate at 533.3 ± 0.15 eV. We conclude that the outermost 10 nm of these fibers, the XPS sampling depth, contain Si and C contributions originating from poly-APS.

Discussion

The topographical, spectroscopic, structural, and mechanical characteristics of the fibers are clear; they have very high aspect ratios (often reaching at least 300) and are flexible, cylindrical, and dominated by crystalline $KHCO_3$ walls. They are typically filled with aqueous KOOCH, and there is evidence for growth by adding $KHCO_3$ to both ends. For 50 nm thick films of poly-APS doped with KOH and CO_2 and spin-coated on SiO_2, nanoribbons, not tubes, are observed.[5] However, 50 nm thick films of undoped poly-APS spin-coated with saturated $KHCO_3$ solution do yield fibers. We propose that the type and extent of structures beneath the film surface vary with film thickness and with salt concentration and composition. The film thickness is an important variable needing further study.

While XPS, EDS, and micro-Raman spectroscopy indicate that the composition of the fiber is dominated by $KHCO_3$, there is evidence from XPS that the outer 10 nm of the fiber contains small amounts of Si (~1 atom %) attributed to poly-APS. EDS detects no Si in the bulk of these fibers, placing an upper limit of ~ 3 atom % Si. Raman data shows no evidence for the Si−O or propyl ($-C_3H_6$) moieties. Thus, at most, minor amounts of poly-APS are involved in the fibers.

On the other hand, poly-APS plays an important role in the fiber growth somewhat analogous to the biomineralization of calcium carbonate ($CaCO_3$).[18,19] In the absence of poly-APS, neither tubes nor nanoribbons form. In considering plausible roles, we first consider the chemistry of poly-APS. The basicity of undoped poly-APS is the result of protonation of the $-NH_2$ groups. Zwitterion formation at the amino propyl group is expected upon exposure to CO_2 and H_2O; that is,

$$\equiv Si-(CH_2)_3-NH_2 + CO_2 \leftrightarrow \equiv Si-(CH_2)_3-NH_2^+COO^- \quad (1)$$

This zwitterion can be deprotonated at the nitrogen by Lewis bases, for example, $-NH_2$ and OH^- ions, the latter generated by equilibration of $-NH_2 + H_2O$.[1] The resulting anionic oligomerized carbamate, $\equiv Si-(CH_2)_3-NHCOO^-$, has been identified in earlier work.[5] Along with this process, poly-APS may catalyze the formation of HCO_3^- and H^+ ions as CO_2 reacts with H_2O.[21] The presence of alkali ions, besides being a prerequisite for salt formation, can also disrupt Si−O−Si bonds to form charged species containing SiO^- and reduce the size of siloxane oligomers. Local assembly, driven by electrostatic forces, of charged small oligomers at the surface of thin poly-APS films has been proposed to account for nanoribbons.[5] However, formate ions ($HCOO^-$), which were not taken into account in previous work,[5] may be a key component in the formation of the nanoribbons as well as the formation of the $KHCO_3$ microfibers. Ionic aggregates of K^+, $HCOO^-$, HCO_3^-, small ionic poly-APS oligomers, and water likely provide the precursor structures that lead to microwells where $KHCO_3$ fibers nucleate and grow.

While many details clearly remain to be explored regarding the fiber nucleation and growth mechanisms, we propose a multistep phenomenological model that accounts for the observed fibers (counterclockwise in Scheme 1). Starting with a K^+/poly-APS solution deposited on SiO_2, we observed the gelation/solidification indicated in step I occurs in less than 12 h and is accompanied by a loss of water and ethanol to form the proposed glassy matrix of poly-APS oligomers and solvated K^+. With time, step II, micron-sized pores and depressions (precursors to microwells) form on the surface of the K^+/poly-APS. In passing, we note that a recent study showed that hole formation on a polymer surface can depend on the relative

(17) A granular $KHCO_3$ sample was exposed to X-ray irradiation for 1 h. The peak at 285 eV (C1s) before and after irradiation remained constant within experimental uncertainty.

(18) Stupp, S. I.; Braum, P. V. *Science* **1997**, *277*, 1242.
(19) Falini, G.; Albeck, S.; Weiner, S.; Addadi, L. *Science* **1996**, *271*, 67.
(20) Silverman, D. N.; Lindskog, S. *Acc. Chem. Res.* **1988**, *21*, 30.
(21) Loerting, T.; Tautermann, C.; Kroemer, R. T.; Kohl, I.; Hallbrucker, A.; Mayer, E.; Liedl, K. R. *Angew. Chem., Int. Ed.* **2000**, *39*, 891.
(22) Thiele, U.; Mertig, M.; Pompe, W. *Phys. Rev. Lett.* **1998**, *80*, 2869.

Scheme 1

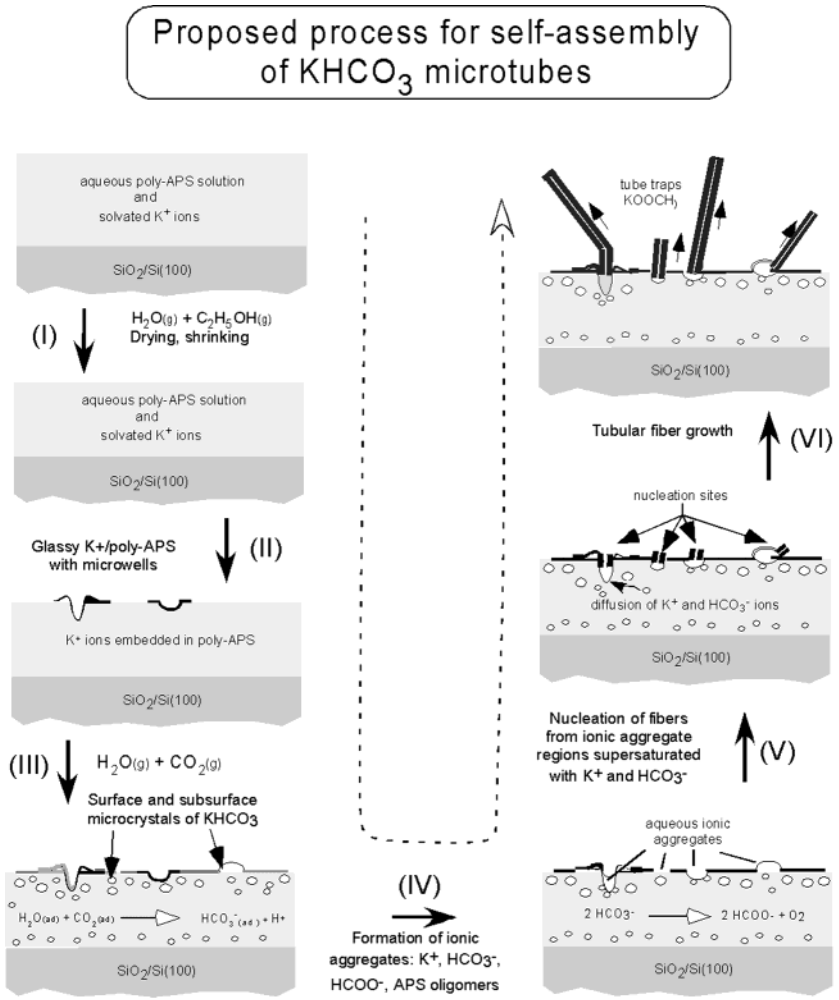

humidity.[22] Subsequent exposure (step III) to $CO_{2(g)}$ and $H_2O_{(l)}$ leads to incorporation that expands and restructures the film. In as little as 4 h, the micron-sized $KHCO_3$ crystals form beneath the film surface. Within 24 h (step IV), some of the HCO_3^- ions convert to $HCOO^-$, a reaction catalyzed by the K^+/poly-APS environment, and aqueous regions form that contain ionic aggregates of K^+, HCO_3^-, $HCOO^-$, and small charged poly-APS oligomers. We propose that the combination of a pore structure in poly-APS, the ionic solution, and water interact to nucleate and grow a fiber (step V). Once nucleated, the length and growth rate are determined by the supply of the ionic fluid from the subsurface region of the film (step VI).

Using this model, the following qualitative picture emerges. We assume a funnel-shaped pore formed by the self-assembly of charged ions derived from the poly-APS is connected to an interconnected void volume region beneath the film surface that contains both microcrystals of $KHCO_3$ and aqueous ionic solution. Emergence of a micron-sized drop of fluid forms a circular moiety. Water loss concentrates the K^+ and HCO_3^-, and $KHCO_3$ crystallizes at the outer edge of the circle. While water is also lost from the center of the droplet, the loss is balanced by the incorporation of water from the ambient by hygroscopic formate and by slowly emerging fluid from within the film.

Once nucleated, growth of high aspect ratio tubes can occur under quasi-static near-equilibrium conditions by adding $KHCO_3$ at either end (step VI). Growth at the base could occur by the arrival of additional fluid at the nucleation site, that is, the base of the funnel of Figure 6. In this mechanism, water is lost at the periphery of the base of the funnel, and crystals form at the outer edge, capturing the fluid inside and extending the length by movement of the solid tube through the surrounding funnel-shaped structure. Alternatively, ionic fluid from the film could move through the internal tube from the base to the terminus where it migrates radially, loses water, and forms $KHCO_3$ at a rate that balances the arrival rate. If the fluid diffuses too slowly in the polymer matrix, the tube growth will stop. If the fluid arrives too rapidly, it will flow laterally across the film surface and, as observed, needlelike crystals will form. When delicately balanced, the tube can continue to grow as long as there is an adequate fluid supply from beneath the surface. It is this delicate balance that must be met and maintained for fiber growth at the outer end.

The K^+ and HCO_3^- ion concentration in the polymeric ionic fluid must be at or near saturation at all times. If the concentration fell below saturation for an extended period, the fiber would dissolve on the poly-APS. If the fluid became supersaturated, the tube would close. The formate ion may play a crucial role in maintaining the necessary control. Account must also be taken of a contribution from the poly-APS that is inferred

(23) Trentler, T. J.; Hickman, K. M.; Goel, S. C.; Viano, A. M.; Gibbons, P. C.; Buhro, W. E. *Science* **1995**, *270*, 1791.

from the XPS data. This component, probably in the form of small ionic oligomers, may be concentrated in the outermost 10 nm of the fibers and serve as a protective layer over the solid $KHCO_3$.

The presence of curved and kinked fibers may be the result of concentration fluctuations, nonuniform radial concentration gradients, and changes in relative humidity. However, the uniform width of the fibers at a kink or along a curved path indicates that these nonuniformities are not vast.

In our growth model, the forces of surface tension play an important role. While these are presently unknown, wetting the inner walls of a preexisting tube of $KHCO_{3(s)}$ with saturated KOOCH would lead to a curved surface at the solid−liquid interface. In this framework, the tube can lengthen until the source of K^+ and HCO_3^- ions is exhausted. We suppose the amount of source materials increases with the thickness of the K^+/poly-APS film. If so, the thin (5 nm) films may possess fluid volumes that are insufficient for nucleation and fiber growth. For the ~40 μm thick films, we find that the volume occupied by the fluid required to grow the fibers is less than 25% of the total film volume. Since the K^+/polyAPS film can continue to take up H_2O and CO_2 from the ambient throughout the whole growth process, the actual void volume for the fluid may be much less.

Related Model. The proposed fiber-forming process has characteristics somewhat analogous to the solution−liquid−solid (SLS) growth mechanism of III−V semiconductor fibers and whiskers recently reported by Trentler et al.[23] The SLS fiber growth method is a modified version of the vapor−liquid−solid (VLS) growth mechanism.[24] In the latter method, for example, a gaseous silicon precursor is absorbed into a metallic nucleation seed (e.g., Au) in the liquid state and is decomposed into free Si atoms to form a Au/Si alloy. At supersaturation, a Si fiber emerges from the droplet and continues to grow as long the Si precursor continues to be supplied. In the SLS method, the nucleation seed and the molecular precursor are in a solution environment, usually in the supercritical state.[25] As noted previously, we propose that saturated aqueous KOOCH in the K^+/poly-APS film, when saturated with K^+ and HCO_3^- ions, serves as the growth medium for $KHCO_3$ fibers.

Extension and Application as a Template. General extension of this work is underway. Replacing K^+ with Na^+, that is, forming Na^+/poly-APS, leads to fiber formation. Although less reproducible, SEM and EDS data show that NaCl fibers (lengths > 50 μm and widths ≈ 0. 50 μm) can be formed from a thin poly-APS film doped with Na^+ and Cl^- ions. This observation points to the importance of structural changes in the poly-APS that occur in the presence of ionic species related to highly soluble salts.

As self-assembled structures, $KHCO_3$ fibers possess several potential advantages; the most noteworthy include built-in error correction, well-defined fibrous structures, and high yields. In addition, the self-assembly process is readily reversible by dissolution in an aqueous environment at room temperature. Thus, $KHCO_3$ microfibers can serve as an easily removed template. For example, we have sputtered deposited Cu onto $KHCO_3$ fibers and dissolved the $KHCO_3$ in water at room temperature. SEM shows that the resulting Cu tubes are, like the templates, high aspect ratio (up to at least 100) and possess a narrow diameter distribution (0.5−3 μm).[26]

Conclusions

We report for the first time the self-assembly of high aspect ratio linear and curved crystalline $KHCO_3$ microfibers formed when a homogeneous aqueous solution of KOH and oligomerized polysiloxane, K^+/poly-APS, is dried under ambient atmosphere conditions to form a glassy film and is then exposed to CO_2 and H_2O. Using XPS, EDS, SEM, and optical and micro-Raman spectroscopies, we conclude that the fibers are narrow (0.5−3 μm), long (aspect ratios up to at least 300), and crystalline cylinders of $KHCO_3$, typically filled with a fluid containing potassium formate. We propose a multistep model in which the poly-APS film assists the formation of fibers by forming microwells filled with an aqueous solution of ionic aggregates, including K^+, HCO_3^-, $HCOO^-$, and small ionic poly-APS oligomers. From such structures, $KHCO_3$ fibers nucleate and grow, a process limited by the supply of saturated K^+ and HCO_3^- formed within the K^+/poly-APS film.

Acknowledgment. This work was supported in part by the National Science Foundation (CHE 0070122). J.M.W. acknowledges support of this work from the Robert A. Welch Foundation (Welch Chair in Chemistry) and by the University of Texas (Center for Materials Chemistry). We also thank Professors Angela Belcher and David Vandenbout for assisting with the optical microscopy.

Supporting Information Available: Optical microscope image of structures on a K^+/poly-APS film exposed to $CO_{2(g)}$ and $H_2O_{(l)}$, SEM micrographs of fibers on poly-APS, SEM image of a bundle of curved fibers transferred from a K^+/poly-APS film onto a highly oriented pyrolytic graphite surface, and energy-dispersive X-ray spectra. This material is available free of charge via the Internet at http://pubs.acs.org.

JA021419N

(24) Westwater, J.; Gossian, D. P.; Tomiya, S.; Ruda, H.; Usui, S. *J. Vac. Sci. Technol., B* **1997**, *15*, 554.
(25) Holmes, J. D.; Johnston, K. P.; Doty, R. C.; Korgel, B. A. *Science* **2000**, *287*, 1471.
(26) Celio, H.; White, J. M. Manuscript in preparation.